Diurnal variations in microbial population dynamics along the human large intestine

Alinaghi Salari[1,2,3] and Jonas Cremer[3*]

[1] Department of Chemistry, University of Toronto, Toronto, ON M5S 3H6, Canada
[2] Terrence Donnelly Centre for Cellular & Biomolecular Research, University of Toronto, Toronto, ON M5S 3E1, Canada
[3] Department of Biology, Stanford University, Stanford, CA 94305, USA
* Corresponding author, jbcremer@stanford.edu

Abstract
The human large intestine contains a highly dynamic microbial ecosystem, where growing cells replenish the biomass regularly lost via feces. Growth is primarily fueled by complex carbohydrates, which enter together with luminal fluids from the small intestine, depending on meal intake and with strong variations throughout the day. To elucidate how these variations shape microbial population dynamics, we introduce a mathematical model incorporating intestinal fluid flow, gut motility, and microbial growth. The model findings demonstrate how the expandable nature of the proximal colon, the presence of a pouch-like cecum, and the periodic exit of luminal contents in large batches in combination maintain a stable microbial population in the proximal large intestine, making it the primary region of microbial growth along the gut. The system promotes an efficient growth filter, fostering the proliferation of fast-growing primary fermenters while washing out slower-growing species. The microbial population also undergoes several daily bottlenecks, resulting in a small effective population size, $N_e \sim 10^7 – 10^{11}$ cells, shaping evolution and competition dynamics. Diurnal fluctuations further cause substantial flow-dependent variations in the host's uptake of fermentation products, the most abundant microbial metabolites constituting an important energy source for the host. These findings underscore the highly intertwined and rapid turnover dynamics of the gut microbiota, set by microbial and host-controlled characteristics, and of preeminent importance for a mechanistic understanding of host-microbiota interactions.

Introduction

The microbial population within the gut strongly influences human physiology, with its size and composition being key factors determining microbe-host interactions.[1–5] However, our understanding of how microbiota size and composition emerge as a complex consequence of food intake, digestion, the active movement of luminal contents, and microbial growth characteristics remains limited, preventing more mechanistic insights into the functioning of this ecosystem and its link with the host.

Along the small intestine, coordinated muscle contractions and a high throughput of water lead to complex flow patterns that promote the efficient uptake of nutrients while preventing strong growth and a substantial accumulation of microbes.[6–8] Gut microbes thus mostly reside in the large intestine (LI), where they form a highly dynamic population in which, fueled by complex dietary carbohydrates not absorbed in the small intestine,[9,10] growing microbes replenish those lost via feces. Importantly, this turnover is rapid as around half of the microbial biomass is being replenished each day, with the exact turnover numbers depending on diet and the active movement of luminal contents (**SI Text 1**). Additionally, nutrient supply and luminal movements vary substantially throughout the day and are tightly coupled to meal intake and digestion activity.[11,12] These diurnal variations and, more generally, the circadian rhythm of the host have been suggested to strongly impact the microbiota and its effect on host physiology.[7,13–16] Overall, microbial cell densities and the total population size of the microbiota in the LI thus emerge from a highly dynamic interplay between nutrient supply, microbial growth, and the active control and flow of luminal contents with possibly strong consequences on the human host.

Different in-vitro setups have been employed to emulate the fundamental principles of microbial growth dynamics and turnover along the LI.[17–20] For instance, microfluidic approaches have been utilized to investigate the interaction of flow and turnover in spatial setups that emulate one or more major characteristics of the intestine, including peristaltic movement, mixing, and interactions between microbiota and the epithelial layer.[21–24] In parallel, mathematical models have been introduced to explore microbial growth and its relation to other dynamics, providing important conceptual insights.[18,22,25] Commonly, microbial growth is studied within a single or a series of well-mixed bioreactors in which inflow and outflow control nutrient supply and turnover.[19,26,27] These studies can provide insight on the fundamental relations between microbial growth, fluid turnover, and microbial density[28] (**SI Text 2** and **Figs. S1 and S2)**. However, these setups and models often do not account for crucial and complex intestinal characteristics, including the strong diurnal fluctuation of flow and nutrient supply, the flexibility of the intestinal volume, and the presence of a cecum as an important growth compartment. Furthermore, bioreactor theory raises the fundamental question of how a stable microbial population can be maintained in bioreactors or the human proximal LI for physiological conditions with very high flow rates (**SI Text 2**).

To unravel microbial growth and population dynamics in the human LI, we here introduce a mathematical modeling framework that integrates key physiological factors, including food intake, digestion, intestinal fluid passage, and microbial growth dynamics. Additionally, we account for the controlled active movement of colonic contents via intestinal muscle contractions

and the turnover of fermentation products (FPs). Following nutrient supply from the small intestine, microbial growth occurs mostly along the proximal LI, including the cecum and the ascending colon. We thus limit our simulations to this region. Through finite-element analysis simulations that reflect the geometry and dynamical processes of the proximal adult human LI, we show how different physiological factors together set microbial population dynamics. The presence of a cecum, the inflow of chyme into the LI peaking after meal intake, and the coordinated abrupt movement of luminal contents towards the distal LI are particularly important in determining microbial population dynamics and their strong fluctuations throughout the day.

Results

A Hydrodynamic Model of Microbial Growth along the Proximal LI

To investigate the growth dynamics of microbes, we set up a model that, following anatomy measurements (**Table S1**), emulates the proximal adult LI (cecum and ascending colon) as a 30-cm long pipe-like structure with a luminal volume of approximately 100 mL (illustration in **Fig. 1A**, **SI Text 3** and **Fig. S3**). We explicitly model the dynamics of nutrient concentrations, $c_n(r, z, t)$, and microbial densities, $c_b(r, z, t)$, in a 2-dimensional axisymmetric domain (coordinates r and z) over time t (**Fig. 1A**, Eqs. 1 and 2). Nutrients, primarily carbohydrates, enter with luminal fluids at the proximal side to support microbial growth (inflow, orange arrow in **Fig. 1A**). Microbes utilize these nutrients and grow with a growth rate depending on the local nutrient concentration and bound below a maximum rate, λ, (Monod kinetics). Microbes and nutrients further move with the flow that emerges from the turnover of intestinal fluids and the mixing of fluids caused by the active contraction of the intestinal walls (i.e., gut motility).[29] Supported by previous in-vitro studies,[25,30] we approximate this movement as an advection-diffusion process with diffusion emulating local mixing (see **SI Text 4**). The drift velocity, $u = (u_r, u_z)$, emerges from the net movement of intestinal fluids, which we account for by the solution of the Navier Stokes equation (**Fig. 1A**, Eq. 3) with appropriate boundary conditions (**Fig. S3**). Following the emerging flow dynamics, unabsorbed nutrients and microbes leave the system at the distal side (outflow, brown arrow in **Fig. 1A**). We use COMSOL Multiphysics to numerically solve the coupled system of equations using its built-in finite element method. As microbial growth parameters (highlighted in green in **Fig. 1A**), we use values observed for the dominant strains of the microbiota composition.[25] Fluid-related parameters (highlighted in blue in **Fig. 1A**) follow different intestinal studies (see **SI Text 4 and 5**). We specifically assume nutrient loads quantified for a British reference diet with an inflow of 1.5 L intestinal fluids per day.[31,32] All parameters used in this study are listed in **Table S1.**

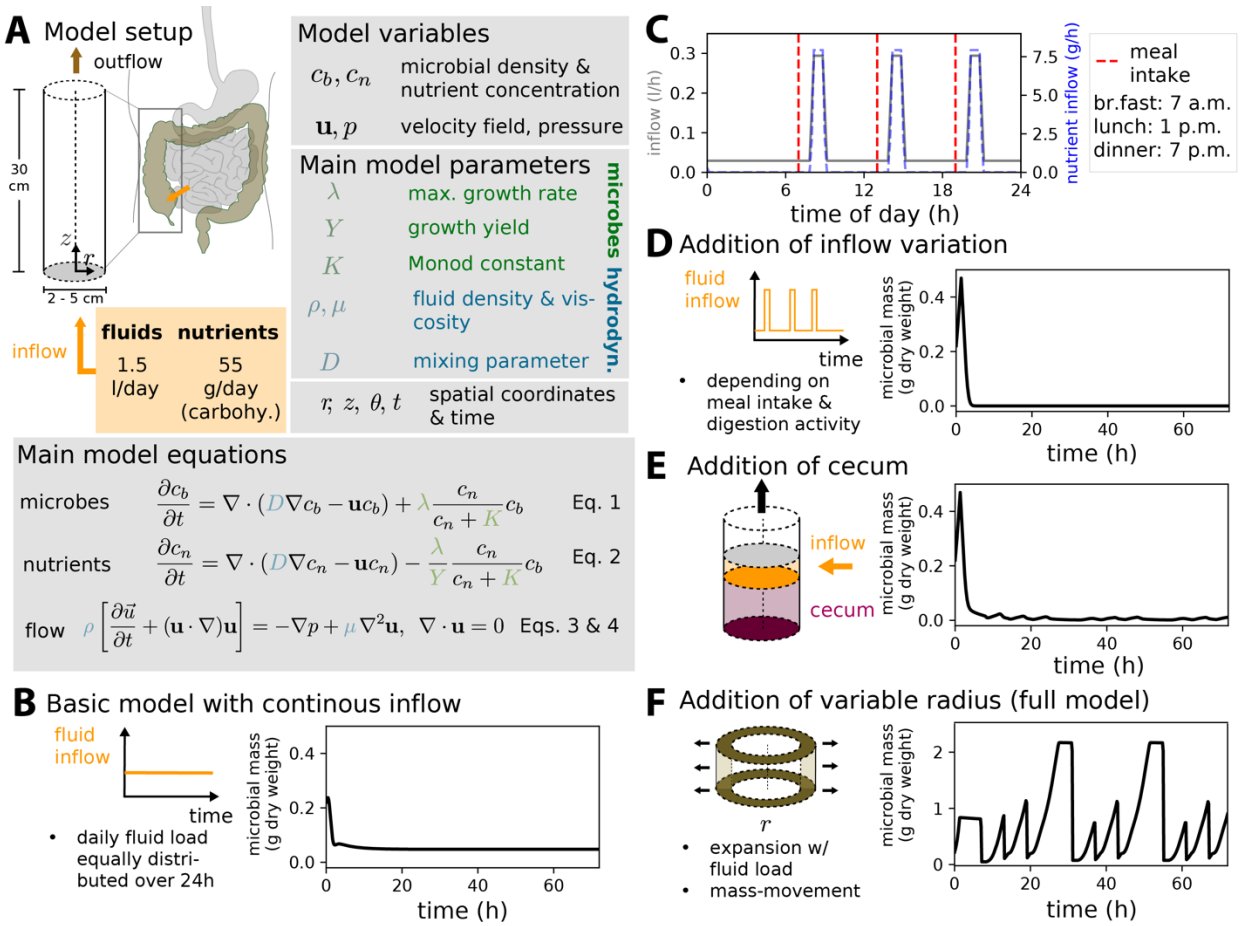

Figure 1. Modeling growth dynamics within the proximal end of the LI indicates dynamical volume changes required for promoting a stable microbial population. (A) Overview of the model setup, equations, and parameters. **(B)** Modeled daily variation of fluid load entering the cecum. **(C)** Basic model considering a pipe-like geometry and a constant daily fluid load entering (net inflow velocity of $u_z \approx 59\ \mu\mathrm{m/s}$ and nutrient concentration of $c_{n_{in}} = 150\ \mathrm{mM}$). The graph shows the change in microbial biomass over 72 h with an initial dry microbe weight of ~ 0.2 g, homogenously distributed throughout the proximal LI. In our simulations, we consider three major meal intakes per day. Based on experimental observations, major peaks of inflow and nutrient concentration arrive at the cecum within 1 h post-meal intake (See **Fig. S4**). **(D-F)** Further extension of the model considering a diurnal varying inflow **(D)**, varying inflow and the presence of cecum **(E)**, and varying inflow and cecum, as well as regular diurnal expansion-contraction cycles of the radius, recapitulating volume control and mass movements along the proximal LI **(F)**. In all scenarios, the same initial conditions as in **C** are used. Used model parameters are provided in **Table S1** with the mixing strength of $D = 10^{-8}\ \mathrm{m^2/s}$. More detailed simulation results for these and other scenarios are provided in **SI Text 6** and **Figs. S5-S9**.

Model Scenarios of Increasing Complexity

To understand how a stable microbial population emerges within the proximal LI despite the presence of strong flow, we start with this most basic model that we subsequently extend in complexity to account for additional key intestinal characteristics.

1. Basic model with constant inflow: We first consider the daily load of 1.5 L luminal fluids entering with a constant rate throughout the day (**Fig. 1B**). The radial variation of flow velocities in the pipe-like geometry, with flow velocities decreasing towards the pipe boundary, is not sufficient to overcome the high throughput of luminal contents and promote a stable microbial population. This is shown by the rapid decrease in population size when starting with a substantial microbial population in the system (**Fig. 1B**).

2. Adding variations in fluid and nutrient inflow: The fluid load entering the LI varies greatly over time, depending on food intake and digestion activities by the host. Measurements of water turnover[31] have shown that the inflow peaks approximately one hour after a major meal intake, while the basal inflow rate in the absence of food intake and digestion is very low or absent (**Fig. S4**), suggesting a highly regulated fluid flow passing the ileocecal valve. Following these observations, we specifically consider a scenario with three major peaks in inflow corresponding to three major meal intakes (**Fig. 1C**). Importantly, this strong variation in flow still does not support higher microbial densities, even throughout the night when the inflow is at its basal rate. The total population size falls to very low levels (**Fig. 1D**).

3. Adding cecum: Next, we consider whether a dead-end, pouch-like cecal compartment can help stabilize microbial densities. To account for the cecum of the human adult, we specifically relocate the ileocecal valve from which nutrients enter to the side of the simulation domain at a 2 cm distance from the proximal end (highlighted in orange in **Fig. 1E**, **SI Text 3** and **Eq. [S16]**). Importantly, while a stable microbial population can persist in the cecum, the addition of a cecum is not sufficient to ensure a high microbial density along the ascending colon, and an initially high abundance of microbes still decreases over time (**Fig. 1E**).

4. Adding dynamical expansion-contraction of the colonic volume: Scintigraphy**,** magnetic resonance imaging measurements, and intervention studies that control fluid and contents inflow into the LI indicate substantial variations in the colonic volume.[33–35] As a prominent controlling mechanism, the gastrocolic reflex, which affects the motility and peristaltic motion of the colon as a result of a stretch of the stomach wall,[36] can lead to the movement of colonic contents in batches, a process often referred to as "mass movement" (**SI Text 5**). Coordinated partially with colonic pressure waves and the sleeping/awakening periods,[37] these contractions appear to be highly dependent on meal intake and the following fluid inflow from the small intestine. To account for a change in the intestinal volume and the temporarily rapid transit of colonic contents, we extend the model to allow for dynamical changes of the intestinal radius r within the observed range of $\sim 1 \leq r \leq \sim 2.7\ \mathrm{cm}$ (**Fig. 1F**; time-dependent colonic radius is shown **in Fig. 2A** below). We specifically model the radius to increase gradually with fluid inflow from the small intestine, while every mass movement leads to a rapid shrinkage in radius. To account for the gastrocolic reflex,[36] we specifically assume the resulting mass movements to

reduce the colonic radius after every meal intake and before substantial fluid loads reach the LI (**See SI - Eqs. [S3]-[S8])**. Importantly, the dynamic adjustment of the radius strongly influences microbial growth and turnover dynamics. As a result, high microbial densities emerge and remain stable (**Fig. 1F**), consistent with observations (see **SI Text 7** for detailed discussion of numbers).[38,39]

In summary, our model connects nutrient supply, flow dynamics, and microbial growth to simulate microbial population dynamics within the proximal LI. Given the high inflow of luminal contents, an expandable volume of proximal LI is required to ensure the observed high microbial densities within that intestinal section.

Diurnal Variations in Growth and Population Size

To better understand the emerging population dynamics and its diurnal variation with meal intake and digestion, we next characterize the full model (scenario 4 discussed above) in more detail. We specifically study the daily variation in radius, microbial load, and nutrient contents over a 24-hour period, following the attainment of a high, albeit fluctuating, microbial population level after a sufficiently long (48 – 72 h) simulation (**Fig. 2**). With meal intake at 7 a.m., mass movements lead to a rapid decrease in the radius (**Fig. 2A**, red arrow), pushing microbes out of the proximal LI and leading to a drop in the total number of microbes (**Fig. 2B**, red arrow). This prepares the colon for the subsequent intake of large amounts of fluids, which enter approximately one hour after meal intake, following digestion in the stomach and small intestine. As the radius begins to increase (**Fig. 2A**, blue arrow), more nutrients enter the intestine, supporting growth (**Fig. 2C**, blue arrow). During this phase, no major outflow occurs (in the simulation, the outflow is assumed to be zero), microbes grow, and the population size increases significantly over time (**Fig. 2B**, black arrow). Similar dynamics (mass movements and subsequent growth phases) repeatedly occur during the rest of the day following two additional meal intakes at 1 p.m. and 7 p.m. After the third meal and during the night, when mass movements are less frequent (no mass movement in the simulations), the microbial population size can increase even higher, resulting in the consumption of all available nutrients (**Fig. 2C**, green arrow).

To further illustrate the dynamics, we next show the spatial variation of microbial density for four time points in the morning (**Fig. 2D**). Notably, the decrease in radius pushes luminal contents with high microbial densities out of the proximal intestine, leaving relatively low densities behind (time points 1 and 2). Local microbial densities become even more depleted with the strong inflow of fluids and nutrients (time point 3). Subsequently, growth leads to a strong increase in microbial densities (time point 4), with microbes from the cecum and distal part repopulating the entire ascending colon (white arrows). The concentration of nutrients follows a reverse trend. Starting with low concentrations, the influx of nutrients after meal intake leads to a strong increase in nutrient concentrations, followed by a subsequent decrease when the density of nutrient-consuming microbial increases (**Fig. 2E**). The full dynamics over a timespan of 24 hours is shown in **Video S1**.

Overall, these findings emphasize highly intertwined population dynamics with strong variations in growth and population size throughout the day, emerging from a tight interplay between meal intake, intestinal fluid turnover, and microbial growth.

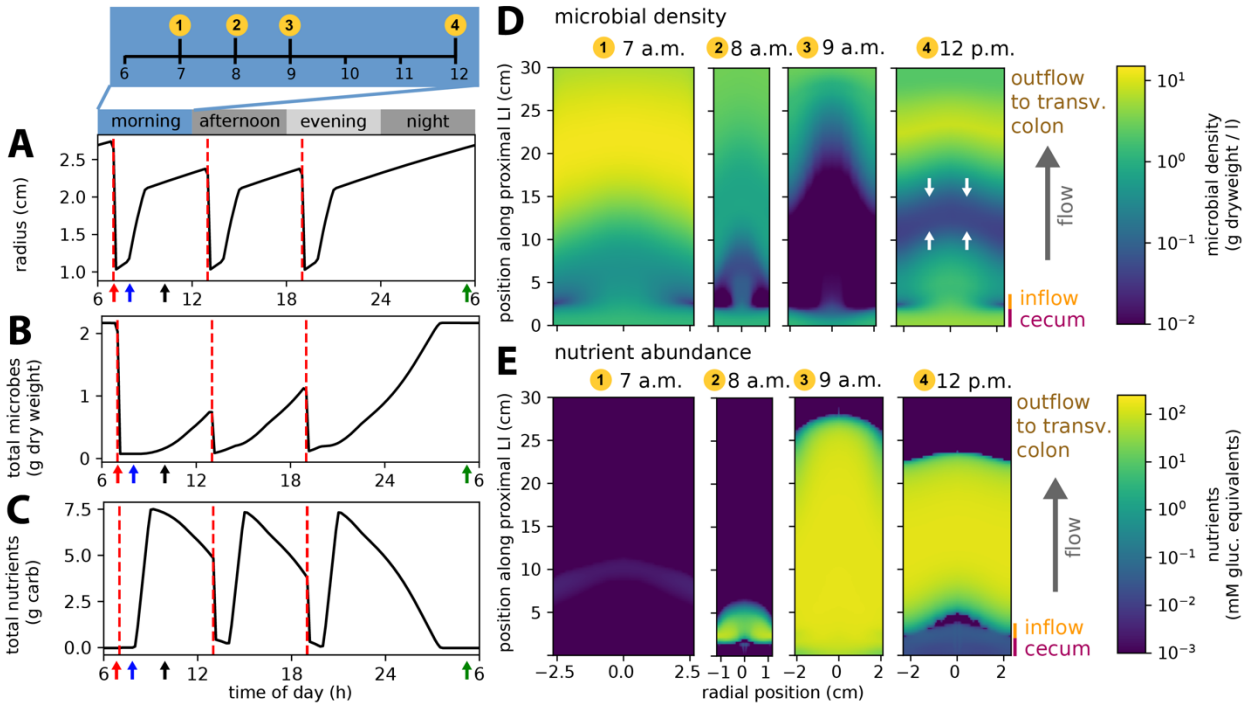

Figure 2. Spatiotemporal growth dynamics. **(A-C)** Temporal variation in radius and the abundance of microbes and nutrients within the proximal LI. The red, blue, black, and green arrows show the timing of the initiation of meal intake and subsequent mass movements, major fluid inflow to the cecum, significant microbial growth phases, and complete nutrient depletion, respectively. **(D, E)** Spatial variation of microbial densities and nutrient concentrations at selected morning time points. The white arrows in (D, E) indicate the two major directions of microbe repopulation in the ascending colon, influenced by a combined effect of growth and diffusion. The presented results reflect a stable microbial population state with recurring daily variations. Full temporal dynamics over 72 h shown in **Fig. S6**. Model parameters are provided in **Table S1**, with the mixing strength of $D = 10^{-8}\ \mathrm{m}^2/\mathrm{s}$. Time-lapsed dynamics are shown in **Video S1**.

Variations in Microbial Growth Rates

To emphasize the consequences of this interplay, we next discuss how variations in the maximum growth rate, λ, affect growth dynamics. The ability of microbial cells to grow largely depends on the coordination of major cellular processes to maintain metabolism and synthesize new proteins and other biomass with strong variations across species.[40,41] For example, primary fermenters utilize carbohydrates and commonly grow rapidly, with doubling times as short as 30 minutes ($\lambda \gtrsim 1.4\ 1/\mathrm{h}$).[9] In contrast, cross-feeding species that use various metabolic strategies to grow anaerobically on FPs, including sulfate reduction[42] and methanogenesis,[43] commonly grow much slower.[44] We, therefore, run simulations for a range of growth rates between $\lambda = 0.2\ 1/\mathrm{h}$ and $1.5\ 1/\mathrm{h}$. Notably, the luminal flow dynamics serve as a "growth filter," with only sufficiently fast-

growing microbes being able to overcome the strong flow and establish a substantial population within the LI (**Figs. 3 and S10**). In addition, flow prevents the accumulation of slow-growing species, including cross-feeding species, which could otherwise consume substantial amounts of FPs released by the primary fermenters. Furthermore, the strong dependence on growth, coupled with the variation in growth behavior across species, emphasizes that changes in microbiota composition— commonly triggered by alterations in diet or antibiotic use— can drastically alter the population size of the microbiota. In summary, these results thus indicate that population dynamics vary substantially with flow conditions, highlighting the host's ability to shape microbial population dynamics and composition.

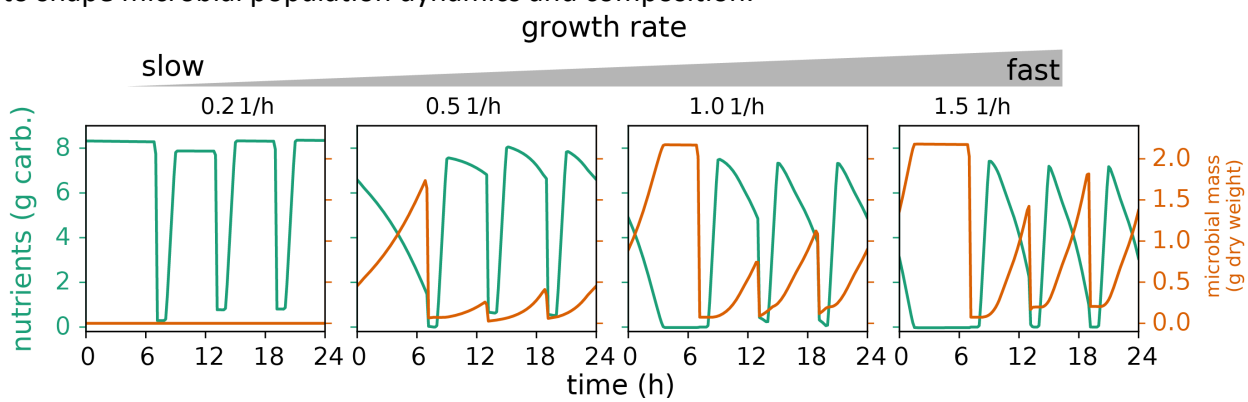

Figure 3. Dependence of microbial abundance on growth behavior. Temporal variation in microbial abundance within the proximal LI for different growth rates, λ, ranging from 0.2 to 1.5 $1/\mathrm{h}$ (corresponding to doubling times between ~ 0.5 h and ~ 3.5 h) with the mixing strength of $D = 10^{-8}\ \mathrm{m}^2/\mathrm{s}$. Other simulation parameters are listed in **Table S1**. See **Fig. S10 for** corresponding kymographs showing spatiotemporal density variations.

Cecum Promotes Growth and Determines Effective Population Size

The number of cells forming a microbial population strongly shapes evolutionary processes. Previous research has highlighted the important role of flow dynamics in setting effective population sizes and thus evolutionary dynamics in gut environments.[30,45] We hence investigate in more detail the consequences of the discussed population dynamics on the number of microbes in the proximal LI. Notably, the microbial population in the cecum promotes growth along the proximal LI after meal intake, as illustrated by a kymograph showing microbial density (**Fig. 4A**) with a rapid drop of microbial density after meal intake (gray arrow) followed by a recovery from the cecum (black arrow). Furthermore, no substantial microbial population remains in simulations without a cecum (**Fig. 4B** dashed line, and **Figs. S9**). The cecal microbial population thus appears to be essential in shaping the population dynamics along the entire proximal LI. The size of the population in the cecum N_{cec} varies strongly over time (**Fig. 4B**, solid line), reaching the lowest values N_{cec}^{min} when the inflow from the small intestine peaks after meal intake and before the cecal population starts repopulating the proximal LI (**Fig. 4B**, markers). With evolution strongly determined by regular bottlenecks in population size [30,45–47] N_{cec}^{min} might be considered as the effective population size N_e of the system, varying between 10^9 and 10^{11} cells, much lower than the $\approx 4 \times 10^{13}$ estimated to populate the entire intestine,[48] and strongly depending on growth and mixing characteristics (**Fig. 4C**). Notably, this number is an upper bound

for the effective population size of gut species as a single species account for only a subfraction of all microbial biomass. For example, for a microbial species accounting for 1% of all microbial cells, the effective population size varies between 10^7 and 10^9 cells. The emptying of the cecal compartment might also be more actively promoted in contrast to what is modeled here, lowering N_{cec}^{min} further. Overall, populations thus undergo strong bottlenecks several times a day with possibly strong effects on evolution.

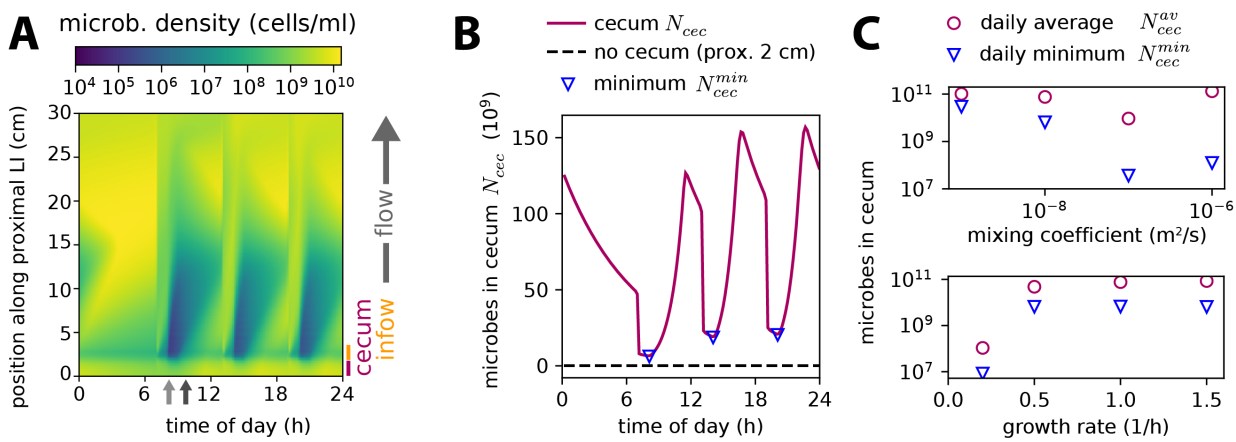

Figure 4. The microbial population in the cecum. (A) Kymograph showing radially averaged microbial density for full model scenario with the cecal compartment. Shortly after a meal intake (gray arrow), the cecal population begins to seed the intestine (black arrow) and thus sets the effective population size (see text). **(B)** Temporal variation in total number of cecal microbes (magenta, N_{cec}). The bottleneck size (triangular markers), shown as minimum population (N_{cec}^{min}), determines the effective population size of the system. For the case with "no cecum", numbers in the proximal 2 cm of the LI are shown. **(C)** Daily average (magenta, represented by N_{cec}^{av}) and minimum (blue) of the cecal microbial population versus variations in mixing conditions (top graph) and microbial growth rates (bottom graph). A growth rate of λ =1 1/h and mixing strength of D = 10^{-8} m^2/s are used in the simulations for the top and bottom graphs, respectively. Additional parameter values are listed in **Table S1**.

Variations in Growth Lead to Variations in the Uptake of Fermentation Products

To further investigate the role of diurnal growth variations for the host, we finally model the fermentation products (FPs) released by primary fermenters to grow within the anoxic environment of the LI. Given the relatively low energy yield of fermentation, microbes release high amounts of FPs; commonly up to about 90% of carbon in complex carbohydrates is released in the form of FPs.[49] Most of the FPs are taken up by the epithelium providing a substantial energy source for the host, 2-12% of the daily energy demand, and impacting many physiological processes[49] (**Fig. 5A**, simulation implementation described in **SI Text 3**). Rates describing the microbial release of FPs, ε_{FP}, and the subsequent uptake per epithelium area, J_{FP}, are taken from culturing experiments[9] and physiological studies of the human LI,[50] respectively. Coupled with microbial growth dynamics, the concentration of FPs in the proximal LI varies significantly throughout the day, with particularly high concentrations during nighttime and low concentrations during daytime (**Fig. 5B**, orange lines). Consequently, the uptake of FPs by the

host also fluctuates strongly (**Fig. 5B**, blue line), leading to a substantial decrease in FPs concentration (**Fig. 5B**, grey lines). Notably, this uptake results in the gradual decrease of FPs across the cross section of the LI, starting at the intestinal wall (**Fig. 5C**), which can impact host uptake. Thus, the uptake rate not only depends on the epithelial uptake capacity, $J_{FP,max}$, but also on the mixing strength, D, of luminal contents (**Fig. 5D**).

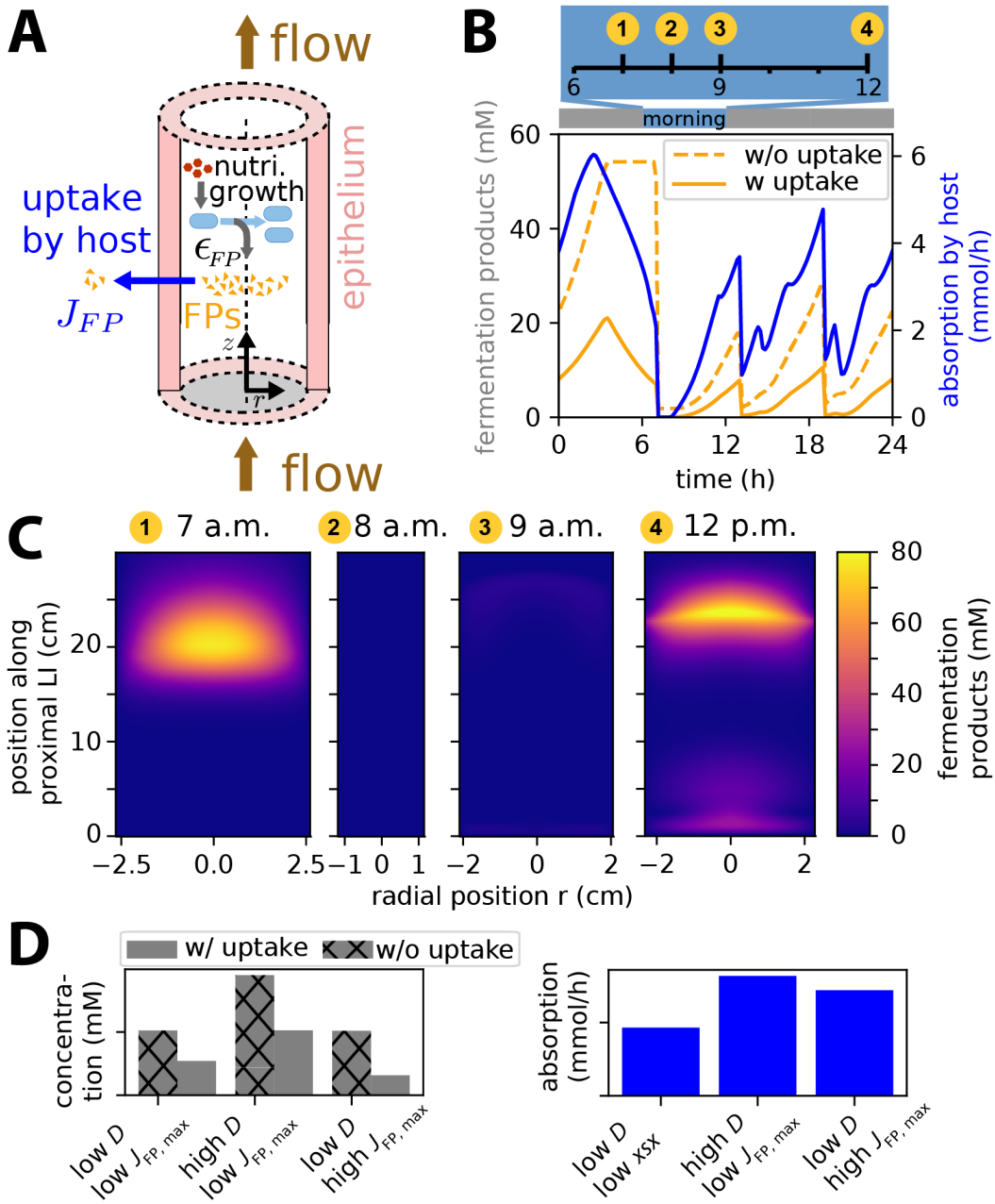

Figure 5. Spatiotemporal variation of microbial FPs. (A) Model incorporating microbial secretion and subsequent uptake of FPs by the host. **(B)** Temporal variation in concentration (orange) and uptake (blue) of FPs along the proximal LI. **(C)** Spatial distribution of FPs concentrations at different times of the morning. Distribution of nutrients and microbes for the corresponding time

points are shown in **Fig. 2D-E**. **(D)** Daily average of concentration and uptake for three different conditions with low and high mixing strengths, $D = 10^{-8}$ and 10^{-6} m^2/s, and low and high maximum uptake rates, $J_{FP,max} = 2.5 \times 10^{-5}$ and $7.5 \times 10^{-5}\ \mathrm{mol}/(\mathrm{m}^2 \cdot \mathrm{s})$. Additional parameter values are listed in **Table S1**. Time-lapsed dynamics are shown in **Video S1**.

Discussion

In this study, we have examined how strong diurnal variations in luminal flow and nutrient supply shape microbial population dynamics along the proximal LI. Through the integrated consideration of flow, mixing, microbial growth, cycles of volume expansion/contraction, and mass movements, our simulation results emphasize significant fluctuations in microbial population sizes throughout the day. Adjustments in the intestinal diameter and the presence of a dead-end cecal compartment, off major flow paths, are essential in ensuring the stable microbial density observed in the proximal LI. Microbial growth rates and the mixing of luminal contents further impact the dynamics, including population bottlenecks and the recovery of microbial populations after large inflow events following meal intakes.

These findings reveal strong consequences on the microbiota and its interaction with the host. For example, the intertwined dynamics discussed here shape evolution simply because of changes in population size alone: Caused by digestion-dependent flow control and nutrient supply, the population cycles through bottlenecks with 10^7 to 10^{10} cells several times a day. Different theoretical and experimental studies have shown that such cycling can strongly shape evolutionary dynamics[46,51,52]. Consider the long-term laboratory evolution experiment by Lenski and colleagues with the model gut bacterium Escherichia coli for illustration.[53] Daily dilution followed by growth leads to the cycling of population sizes with a bottleneck size of 10^7, comparable to the population size bottlenecks in the gut, and with well-established consequences of these bottlenecks on evolution.[46,47]

Another consequence is the limitation of cross-feeding on lower trophic levels: To metabolically utilize microbial excretion products in the anoxic environment of the gut, cross-feeding strains need to employ metabolic strategies alternative to fermentation, such as sulfate reduction or methanogenesis[42]. However, those strategies typically incur a high metabolic burden and result in substantially slower growth compared to primary fermenters.[43] Given the strong flow, these cross-feeders can thus not accumulate along the proximal intestine, and microbial metabolites and other excretion products are instead mostly taken up by the host to serve as energy sources and signaling factors.[9] Furthermore, as the microbial secretion of FPs varies with nutrient availability throughout the day, their uptake by the host can also vary strongly, with possible impacts on host physiology and behavior, such as hunger and satiety control.[54]

Finally, the simulation results also emphasize the host's various abilities to control and adjust microbial population dynamics, for example, via the regulation of luminal water turnover, the adjustment of mass movements, and the mixing of luminal contents. As such, our analysis underscores highly intertwined population dynamics, shaped by the interplay of growth, flow dynamics, and the evolved physiological processes, essential to consider for gaining a more mechanistic understanding of microbe-host interactions.

We based our modeling framework on the current physiological understanding of the large intestine, focusing on the most important processes. This provided new insights into the functioning of the human microbiota not possible with other approaches, like studies with animal models. But naturally, this modeling approach also comes with its own limitations as it needs to simplify many complex host processes. Future in-vitro experiments, in-vivo studies, and extended modeling are thus needed to probe model predictions and better elucidate the discussed intertwined dynamics and their feedback with other intestinal processes. For example, the release of FPs at high levels is known to acidify the luminal environment, which can differentially slow down the growth of various species, further linking microbiota composition to nutrient intake and flow.[25,55] The diurnal variations in nutrient availability, microbial growth, and FPs turnover discussed in this study are expected to shape this interplay, with strong consequences for microbiota composition. Similarly, the differential utilization of different nutrients might lead to a substantial variation in growth behavior, which, given the close connection between growth and population dynamics, not only shapes composition but also the absolute numbers of microbial cells. Finally, we think the role of the vermiform appendix should be further explored. It has been previously suggested to serve as a safehouse for promoting a stable recovery of the microbiota after drastic disruptions, such as diarrhea or antibiotics treatment.[56–58] Given the regular cycling of the microbiota through relatively small population sizes discussed in this study, the presence of a substantial microbial population in the appendix,[56,59] and the observed changes in microbiota composition after appendectomy,[58] future investigations might reveal a more continuous role of the vermiform appendix in controlling and stabilizing the gut microbiota on a daily basis.

Author Contributions

A.S. and J.C. developed the research project, analyzed and discussed the data, and wrote the manuscript. A.S. implemented and ran the finite-element simulations.

Acknowledgment

We thank Markus Arnoldini, Benjamin Good, and members of the Cremer group for critical reading and suggestions to improve the manuscript.

Funding

J.C. acknowledges support from a Stanford Bio-X Seeding Grant (grant number 10-32) and a Terman fellowship.

Code and Data Availability

A simulation file to run COMSOL Multiphysics simulations, including different elements of the model, is available on the GitHub repository accessible via the website https://github.com/cremerlab/diurnal_growthvariations. This repository also contains the Python code to analyze simulation results and generate figures.

References

1. Lozupone, C. A., Stombaugh, J. I., Gordon, J. I., Jansson, J. K. & Knight, R. Diversity, stability and resilience of the human gut microbiota. *Nature* **489**, 220–230 (2012).
2. Marchesi, J. R. *et al.* The gut microbiota and host health: A new clinical frontier. *Gut* **65**, 330–339 (2016).
3. Hou, K. *et al.* Microbiota in health and diseases. *Signal Transduct. Target. Ther.* **7**, 135 (2022).
4. Lloyd-Price, J. *et al.* Multi-omics of the gut microbial ecosystem in inflammatory bowel diseases. *Nature* **569**, 655–662 (2019).
5. Vandeputte, D. *et al.* Quantitative microbiome profiling links gut community variation to microbial load. *Nature* **551**, 507–511 (2017).
6. Codutti, A., Cremer, J. & Alim, K. Changing flows balance nutrient absorption and bacterial growth along the gut. *Phys. Rev. Lett.* **129**, 138101 (2022).
7. Bishehsari, F., Voigt, R. M. & Keshavarzian, A. Circadian rhythms and the gut microbiota: from the metabolic syndrome to cancer. *Nat. Rev. Endocrinol.* (2020).
8. Thaiss, C. A. *et al.* Microbiota diurnal rhythmicity programs host transcriptome oscillations. *Cell* **167**, 1495-1510.e12 (2016).
9. Arnoldini, M. *et al.* Quantifying the daily harvest of fermentation products from the human gut microbiota. *bioRxive* (2024).
10. Cummings, J. H. & Englyst, H. N. Fermentation in the human large intestine and the available substrates. *Am. J. Clin. Nutr.* **45**, 1243–1255 (1987).
11. Hammer, J. & Phillips, S. F. Fluid loading of the human colon: Effects on segmental transit and stool composition. *Gastroenterology* **105**, 988–998 (1993).

12. Karaus, M. & Wienbeck, M. Colonic motility in humans-a growing understanding. *Baillieres Clin. Gastroenterol.* **5**, 453–478 (1991).
13. Wang, H., Zhang, H. & Su, Y. New insights into the diurnal rhythmicity of gut microbiota and its crosstalk with host circadian rhythm. *Animals* **12**, 1–13 (2022).
14. Zarrinpar, A., Chaix, A., Yooseph, S. & Panda, S. Diet and feeding pattern affect the diurnal dynamics of the gut microbiome. *Cell Metab.* **20**, 1006–1017 (2014).
15. Dantas Machado, A. C. *et al.* Diet and feeding pattern modulate diurnal dynamics of the ileal microbiome and transcriptome. *Cell Rep.* **40**, 111008 (2022).
16. Alvarez, Y., Glotfelty, L. G., Blank, N., Dohnalová, L. & Thaiss, C. A. The microbiome as a circadian coordinator of metabolism. *Endocrinology* **161**, bqaa059 (2020).
17. Renwick, S. *et al.* Culturing human gut microbiomes in the laboratory. *Annu. Rev. Microbiol.* **75**, 49–69 (2021).
18. Labarthe, S. *et al.* A mathematical model to investigate the key drivers of the biogeography of the colon microbiota. *J. Theor. Biol.* **462**, 552–581 (2019).
19. Habib, S., Swaby, A. M., Gaisawat, M. B., Kubow, S. & Agellon, L. B. A novel, scalable, and modular bioreactor design for dynamic simulation of the digestive tract. *Biotechnol. Bioeng.* **118**, 4338–4346 (2021).
20. Roupar, D. *et al.* Bioengineering approaches to simulate human colon microbiome ecosystem. *Trends Food Sci. Technol.* **112**, 808–822 (2021).
21. Pimenta, J. *et al.* Organ-on-chip approaches for intestinal 3D in vitro modeling. *Cmgh* **13**, 351–367 (2022).

22. Cremer, J. *et al.* Effect of flow and peristaltic mixing on bacterial growth in a gut-like channel. *Proc. Natl. Acad. Sci. U. S. A.* **113**, 11414–11419 (2016).

23. Kim, H. J., Huh, D., Hamilton, G. & Ingber, D. E. Human gut-on-a-chip inhabited by microbial flora that experiences intestinal peristalsis-like motions and flow. *Lab. Chip* **12**, 2165–2174 (2012).

24. Ashammakhi, N. *et al.* Gut-on-a-chip: Current progress and future opportunities. *Biomaterials* **255**, 120196 (2020).

25. Cremer, J., Arnoldini, M. & Hwa, T. Effect of water flow and chemical environment on microbiota growth and composition in the human colon. *Proc. Natl. Acad. Sci. U. S. A.* **114**, 6438–6443 (2017).

26. Macfarlane, G. T., Macfarlane, S. & Gibson, G. R. Validation of a three-stage compound continuous culture system for investigating the effect of retention time on the ecology and metabolism of bacteria in the human colon. *Microb. Ecol.* **35**, 180–187 (1998).

27. Venema, K. & Van Den Abbeele, P. Experimental models of the gut microbiome. *Best Pract. Res. Clin. Gastroenterol.* **27**, 115–126 (2013).

28. Penry, D. L. & Jumars, P. A. Modeling animal guts as chemical reactors. *Am. Nat.* **129**, 69–96 (1987).

29. Chaudhary, N. A. & Truelove, S. C. Colonic motility. A critical review of methods and results. *Am. J. Med.* **31**, 86–106 (1961).

30. Labavić, D., Loverdo, C. & Bitbol, A. F. Hydrodynamic flow and concentration gradients in the gut enhance neutral bacterial diversity. *Proc. Natl. Acad. Sci. U. S. A.* **119**, (2022).

31. Phillips, S. F. & Giller, J. The contribution of the colon to electrolyte and water conservation in man. *J. Lab. Clin. Med.* **81**, 733–746 (1973).

32. Debongnie, J. C. & Phillips, S. F. Capacity of the human colon to absorb fluid. *Gastroenterology* **74**, 698–703 (1978).

33. Spiller, R. C., Brown, M. L. & Phillips, S. F. Decreased fluid tolerance, accelerated transit, and abnormal motility of the human colon induced by oleic acid. *Gastroenterology* **91**, 100–107 (1986).

34. Kamath, P. S., Phillips, S. F., O'Connor, M. K., Brown, M. L. & Zinsmeister, A. R. Colonic capacitance and transit in man: modulation by luminal contents and drugs. *Gut* **31**, 443–449 (1990).

35. Pritchard, S. E. *et al.* Fasting and postprandial volumes of the undisturbed colon: Normal values and changes in diarrhea-predominant irritable bowel syndrome measured using serial MRI. *Neurogastroenterol. Motil.* **26**, 124–130 (2014).

36. Malone, J. C. & Thavamani, A. Physiology, Gastrocolic reflex. *StatPearls* **29**, 31751078 (2019).

37. Narducci, F., Bassotti, G., Gaburri, M. & Morelli, A. Twenty four hour manometric recording of colonic motor activity in healthy man. *Gut* **28**, 17–25 (1987).

38. Marteau, P. *et al.* Comparative study of bacterial groups within the human cecal and fecal microbiota. *Appl. Environ. Microbiol.* **67**, 4939–4942 (2001).

39. Gorbach, S. L. *et al.* Studies of intestinal microflora. II. Microorganisms of the small intestine and their relations to oral and fecal flora. *Gastroenterology* **53**, 856–867 (1967).

40. Scott, M. & Hwa, T. Shaping bacterial gene expression by physiological and proteome allocation constraints. *Nat. Rev. Microbiol.* **21**, 327–342 (2023).

41. Chure, G. & Cremer, J. An optimal regulation of fluxes dictates microbial growth in and out of steady state. *eLife* **12**, e84878 (2023).

42. Gibson, G. R., Macfarlane, G. T. & Cummings, J. H. Sulphate reducing bacteria and hydrogen metabolism in the human large intestine. *Gut* **34**, 437–439 (1993).

43. Müller, A. L. *et al.* An alternative resource allocation strategy in the chemolithoautotrophic archaeon *Methanococcus maripaludis*. *Proc. Natl. Acad. Sci.* **118**, e2025854118 (2021).

44. Gibson, G. R., Cummings, J. H. & Macfarlane, G. T. Growth and activities of sulphate-reducing bacteria in gut contents of healthy subjects and patients with ulcerative colitis. *FEMS Microbiol. Lett.* **86**, 103–112 (1991).

45. Ghosh, O. M. & Good, B. H. Emergent evolutionary forces in spatial models of luminal growth and their application to the human gut microbiota. *Proc. Natl. Acad. Sci.* **119**, e2114931119 (2022).

46. Izutsu, M., Lake, D. M., Matson, Z. W. D., Dodson, J. P. & Lenski, R. E. Effects of periodic bottlenecks on the dynamics of adaptive evolution in microbial populations. *biorxiv* (2021).

47. Good, B. H., McDonald, M. J., Barrick, J. E., Lenski, R. E. & Desai, M. M. The dynamics of molecular evolution over 60,000 generations. *Nature* **551**, 45–50 (2017).

48. Sender, R., Fuchs, S. & Milo, R. Revised estimates for the number of human and bacteria cells in the body. *PLoS Biol.* **14**, 1–14 (2016).

49. Den Besten, G. *et al.* The role of short-chain fatty acids in the interplay between diet, gut microbiota, and host energy metabolism. *J. Lipid Res.* **54**, 2325–2340 (2013).

50. McNeil, N. I., Cummings, J. H. & James, W. P. T. Short chain fatty acid absorption by the human large intestine. *Gut* **19**, 819–822 (1978).

51. Cvijović, I., Good, B. H., Jerison, E. R. & Desai, M. M. Fate of a mutation in a fluctuating environment. *Proc. Natl. Acad. Sci.* **112**, (2015).

52. Otto, S. P. & Whitlock, M. C. The probability of fixation in populations of changing size. *Genetics* **146**, 723–733 (1997).

53. Lenski, R. E., Rose, M. R., Simpson, S. C. & Tadler, S. C. Long-term experimental evolution in escherichia coli. I. Adaptation and divergence during 2,000 generations. *Am. Nat.* **138**, 1315–1341 (1991).

54. Bastings, J. J. A. J., Venema, K., Blaak, E. E. & Adam, T. C. Influence of the gut microbiota on satiety signaling. *Trends Endocrinol. Metab.* **34**, 243–255 (2023).

55. Walker, A. W., Duncan, S. H., McWilliam Leitch, E. C., Child, M. W. & Flint, H. J. pH and peptide supply can radically alter bacterial populations and short-chain fatty acid ratios within microbial communities from the human colon. *Appl. Environ. Microbiol.* **71**, 3692–3700 (2005).

56. Randal Bollinger, R., Barbas, A. S., Bush, E. L., Lin, S. S. & Parker, W. Biofilms in the large bowel suggest an apparent function of the human vermiform appendix. *J. Theor. Biol.* **249**, 826–831 (2007).

57. Killinger, B. & Labrie, V. The appendix in Parkinson's disease: From vestigial remnant to vital organ? *J. Park. Dis.* **9**, S345–S358 (2019).

58. Cai, S. *et al.* Appendectomy is associated with alteration of human gut bacterial and fungal communities. *Front. Microbiol.* **12**, 724980 (2021).

59. Guinane, C. M. *et al.* Microbial composition of human appendices from patients following appendectomy. *mBio* **4**, 1–6 (2013).